Effects of External Protons on Single Cardiac Sodium Channels from Guinea Pig Ventricular Myocytes

JI-FANG ZHANG and STEVEN A. SIEGELBAUM

From the Department of Pharmacology, Center for Neurobiology and Behavior, Howard Hughes Medical Institute, Columbia University, New York 10032

ABSTRACT The effects of external protons on single sodium channel currents recorded from cell-attached patches on guinea pig ventricular myocytes were investigated. Extracellular protons reduce single channel current amplitude in a dose-dependent manner, consistent with a simple rapid channel block model where protons bind to a site within the channel with an apparent pK_H of 5.10. The reduction in single channel current amplitude by protons is voltage independent between −70 and −20 mV. Increasing external proton concentration also shifts channel gating parameters to more positive voltages, consistent with previous macroscopic results. Similar voltage shifts are seen in the steady-state inactivation (h_∞) curve, the time constant for macroscopic current inactivation (τ_h), and the first latency function describing channel activation. As pH_o decreases from 7.4 to 5.5, the midpoint of the h_∞ curve shifts from −107.6 ± 2.6 mV (mean ± SD, $n = 16$) to −94.3 ± 1.9 mV ($n = 3$, $P < 0.001$). These effects on channel gating are consistent with a reduction in negative surface potential due to titration of negative external surface charge. The Gouy-Chapman-Stern surface charge model incorporating specific proton binding provides an excellent fit to the dose–response curve for the shift in the midpoint of the h_∞ curve with protons, yielding an estimate for total negative surface charge density of −1e/490 Å^2 and a pK_H for proton binding of 5.16. By reducing external surface Na^+ concentration, titration of negative surface charge can also quantitatively account for the reduction in single Na^+ channel current amplitude, although we cannot rule out a potential role for channel block. Thus, titration by protons of a single class of negatively charged sites may account for effects on both single channel current amplitude and gating.

INTRODUCTION

Although the inhibitory effects of extracellular protons on macroscopic sodium current in nerve and muscle cells have been well known since the initial observations of Hille (1968), the single channel basis for these effects remains uncertain. From studies on macroscopic sodium currents in nerve (Hille, 1968; Drouin and The, 1969; Woodhull, 1973; Begenisich and Danko, 1983), skeletal muscle (Campbell,

Dr. Zhang's present address is Department of Molecular and Cellular Physiology, Beckman Center, Stanford University, Stanford, CA 94305.

J. GEN. PHYSIOL. © The Rockefeller University Press · 0022-1295/91/12/1065/19 $2.00
Volume 98 December 1991 1065–1083

1982), and cardiac muscle (Yatani, Brown, and Akaike, 1984), it is generally agreed that increasing the external proton concentration has two main actions: it causes a shift in channel gating to more positive potentials and reduces the maximal sodium conductance. While the shift in gating is commonly thought to result from titration of external negative surface charges, the mechanism for the decrease in peak sodium conductance remains uncertain (see Hille, 1984).

Three main models have been proposed to account for the reduction in peak sodium conductance. According to the channel block model proposed by Woodhull (1973; see also Begenisich and Danko, 1983; Mozhayeva, Naumov, and Nosyreva, 1984), protons bind to a site inside the channel and block ionic current flow. Since the binding site lies within the membrane electric field, the block is voltage dependent. This hypothesis was challenged by Campbell (1982), who showed a voltage-independent reduction of sodium tail currents by external protons. This led Campbell to propose a second hypothesis: that the apparent voltage-dependent block of peak Na^+ current is due to a proton-dependent modification of channel gating. Third, Drouin and Neumcke (1974) have suggested that protons, by titrating external negative surface charge, reduce the local Na^+ concentration near the entrance to the pore, thereby decreasing the Na^+ current magnitude. Using noise analysis of the macroscopic sodium current, Sigworth (1980) showed that reducing external pH reduces single sodium channel conductance, consistent with channel block or surface charge models.

To distinguish more directly between effects of protons on gating and on single channel conductance, we have studied the effects of external protons on single sodium channel currents from guinea pig ventricular myocytes. We report here that external protons both reduce the single sodium channel current amplitude and shift the voltage dependence of channel gating to more positive potentials. Both the reduction in single channel current amplitude and the shift in gating can be explained by the titration of a single class of negative surface charges in a voltage-independent manner, although our data do not rule out a role for channel block.

Some of our results have appeared in abstract form (Zhang and Siegelbaum, 1990).

METHODS

Preparation and Solutions

Single cardiac myocytes were obtained from guinea pig ventricle by the method of Isenberg and Klockner (1982) with slight modifications (Binah, Rubinstein, and Gilat, 1987). Briefly, guinea pigs (200–250 g) were anesthetized with pentobarbitone sodium, their hearts removed quickly, and the aortas cannulated and retrogradely perfused with the following series of solutions bubbled with 100% O_2: (*1*) a normal Tyrode's solution containing (in mM) 140 NaCl, 4 KCl, 1 $MgCl_2$, 5 HEPES, 1.8 $CaCl_2$, and 10 glucose at pH 7.4; (*2*) a Ca-free Tyrode's solution; (*3*) a collagenase solution (type I collagenase [Sigma Chemical Co., St. Louis, MO] in Ca-free Tyrode's solution); and (*4*) KB solution containing (in mM) 70 KCl, 0.5 EGTA, 20 taurine, 20 glucose, 5 creatine, 30 K_2HPO_4, 5 pyruvic acid, 5 $MgSO_4$, 5 Na_2ATP, and 0.12 $CaCl_2$ at pH 7.4. Normally, cells were stored in the KB solution and used within 10 h.

During the experiment, the cell membrane potential was zeroed with a high potassium solution containing (in mM): 25 KCl, 120 potassium glutamate, 0.8 $MgCl_2$, 1 EGTA, 10 HEPES,

and 10 glucose. In all experiments, the pH of the bath solution was kept at 7.4. The pipette was filled with a modified sodium Tyrode's solution containing (in mM): 145 NaCl, 4 KCl, 2 $CaCl_2$, 0.8 $MgCl_2$, and 10 HEPES at pH 7.4. Where necessary, HEPES was substituted with the same amount of the following buffers for different values of pH: MES (2-[*N*-morpholino]ethanesulfonic acid; pK = 6.1) and CAPS (3-[cyclohexylamino]-1-propane-sulfonic acid; pK = 10.4). Unless otherwise specified, the pH value (pH_o) refers to that of the pipette solution. Control experiments showed that reduced single channel current amplitude at lower pH_o is not due to block by the buffer used to adjust pH. All experiments were performed at room temperature (19–21°C).

Experimental Protocols

Patch pipettes were fabricated from 1211-M capillary tubes (Glass Company of America, Millville, NJ) by a standard two-stage pull with a Narishige puller (Narishige USA, Inc., Greenvale, NY). The pipettes were coated with one layer of Sylgard (Dow Corning 184) and fire-polished right before an experiment. Small pipette diameters, with resistances between 10 and 30 MΩ, were used to obtain patches with only a small number (one to four) of channels.

Single channel currents were recorded from cell-attached patches using an EPC-7 patch-clamp amplifier (List Biological Laboratories, Inc., Campbell, CA) (Hamill, Marty, Neher, Sakmann, and Sigworth, 1981). The output of the amplifier was filtered at 2.0 kHz (3 dB down) with an 8-pole bessel filter (Frequency Devices Inc., Haverhill, MA). Command voltage clamp pulses were applied using a DEC LSI 11/73 computer with an INDEC Systems (Sunnyvale, CA) laboratory interface. Data were sampled at 10 kHz using a 12-bit A/D converter and stored on hard disk for analysis.

40-ms-long step depolarizations were applied to the patches from negative holding potentials to test potentials between −70 and −20 mV at a rate of 1 Hz. For multi-channel patches, the holding potential for each test potential was chosen to inactivate a significant fraction of channels in the patch to minimize the number of overlapping openings and to obtain an adequate number of sweeps with no openings (null sweeps). In cases where the number of channels was less than three, the holding potential was set at or negative to −120 mV to eliminate resting inactivation.

Steady-state inactivation curves were obtained by holding the patch at a series of different potentials (−140 to −60 mV) and stepping to a constant test potential (normally −40 mV, except at pH_o 4.3, where the test potential was −20 mV). Peak normalized ensemble-averaged currents were fitted by a Hodgkin-Huxley inactivation curve of the form:

$$h_\infty = \frac{1}{1 + \exp\left(\frac{V - V_{1/2}}{k}\right)} \tag{1}$$

where $V_{1/2}$ is the midpoint of the steady-state inactivation curve and k is the slope factor. The declining phase of the ensemble-averaged currents is usually fitted by a single exponential function to obtain the time constant of inactivation of the ensemble-averaged current (τ_h).

Single Channel Analysis

Details of single channel analysis and the related theory have been presented (Berman, Camardo, Robinson, and Siegelbaum, 1989). Briefly, linear leak and capacitative currents were subtracted from all records. Idealized records were analyzed using a half-amplitude event detection routine (Colquhoun and Sigworth, 1983). A linear interpolation was used between data points just above and below the threshold to define the transition time at a nominal resolution of twice the sampling frequency. In cases where there were overlapping openings, a

particular closing was assigned to a particular opening using a random number generator (valid as long as events are independent).

Histograms of single channel current amplitude, open time, closed time, and first latency to opening distributions were fitted using the method of maximum likelihood and a simplex algorithm. Single channel current amplitude histograms were fitted by Gaussian distributions. Usually, two peaks were resolved. Since the smaller peak accounted for $<10\%$ of the area, values from the dominant peak were used. Open-time histograms ($o(t)$) were generally fitted by a single exponential function to obtain the mean channel open time (τ_o). Closed time histograms and cumulative first latency distributions $P_1(t)$ (i.e., the probability that the first opening in a sweep occurs after time t) were fitted by the sum of two exponential functions. Events shorter than 200 μs were ignored in the fitting and the fits were corrected for these missed events. The conditional probability, $m(t)$, that a channel is open at time t given that it opens at time 0, was obtained by synchronizing all records at the time of the first opening and averaging them. When possible, data were also fitted by the Aldrich-Corey-Stevens (1983) model to calculate the rate constants.

Theory

Surface potential effects. To relate surface potential to changes in external pH, we used the Gouy-Chapman-Stern model, which includes effects of charge screening and the specific binding of protons to fixed negative surface charges (e.g., Hille, 1984). This model uses the Grahame equation (Grahame, 1947) to relate membrane surface potential to free surface charge density:

$$\sigma^2 = 2\epsilon\epsilon_o RT \sum_i c_i \left[\exp\left(-\frac{z_i \psi_o F}{RT}\right) - 1\right] \tag{2}$$

where σ is the free surface charge density, ϵ is the dielectric constant for aqueous solution, ϵ_o is the polarizability of free space, c_i is the concentration of the ith ion in the bulk solution, z_i is the valence, ψ_o is the surface potential, and RT/F is 25.26 mV at 20°C. For a given proton concentration, the free (unprotonated) surface charge density is related to total surface charge density, σ_t, by a simple one-to-one binding equation:

$$\sigma = \frac{\sigma_t}{1 + \dfrac{[H]_m}{K_H}} \tag{3}$$

where K_H is the apparent dissociation constant of protons for the binding site and $[H]_m$ is the proton concentration at the membrane surface and is related to the proton concentration in the bulk solution, $[H]_o$, through the Boltzmann equation:

$$[H]_m = [H]_0 \exp\left(-\frac{\psi_0 F}{RT}\right) \tag{4}$$

A Newton-Raphson iteration procedure (Dorn and McCracken, 1972; Krafte and Kass, 1988) was used to solve Eqs. 2–4 to estimate the surface potential at a given pH_o. Values for σ_t and K_H were then obtained by fitting models that incorporate the surface potential effects (see below) with Eqs. 2–4 using a nonlinear least-squares simplex routine.

Effects on single channel current amplitude. Three models were used to describe the inhibitory effects of protons on single channel current amplitude, i. Model 1 is a simple one-to-one binding scheme (which ignores surface charge effects) where a proton binds to a site in the channel and completely blocks current flow on a rapid time scale, causing an apparent

reduction in i, yielding:

$$i = \frac{i_{max}}{1 + \frac{[H]}{K_H^*}} \tag{5}$$

where K_H^* is the dissociation constant for binding to the channel, i_{max} is the maximal current with no block, and $[H]$ is the proton concentration in the bulk solution.

Model 2 is a modified channel block model which includes effects of negative surface charge on the local proton concentration at the binding site. It is given by a modified version of Eq. 5 where $[H]$ is replaced by $[H]_m$, the proton concentration at the external membrane surface (given by Eq. 4). Model 2 has four free parameters, σ_t, i_{max}, K_H, and K_H^*, and was fit to the dose–response data using a simplex routine and Eqs. 2–5.

Model 3 assumes that the decrease in single channel current with protons is due to a reduction in local Na^+ concentration at the membrane surface. We have modeled the effects of reduced local sodium concentration in two ways. In the simplest approach (model 3A), we assume that the sodium current is simply proportional to local $[Na^+]_o$, and that local $[Na^+]_o$ is related to bulk $[Na^+]_o$ by the Boltzmann equation, analogous to Eq. 4. This yields the following expression:

$$i = i' \exp\left(-\frac{\psi_o F}{RT}\right) \tag{6}$$

where i' is the current when the surface potential is 0 mV. Model 3A was fitted to the dose–response data using Eqs. 2–4 and 6. In a second approach (model 3B) we used the Goldman-Hodgkin-Katz equation, modified for surface potential effects, to calculate single channel current:

$$i = \frac{P_{Na}(E - \psi_o) F^2}{RT} \cdot \frac{Na_i - Na_o \exp\left(-\frac{FE}{RT}\right)}{1 - \exp\left(-\frac{F(E - \psi_o)}{RT}\right)} \tag{7}$$

The results of the fits were compared using the F-test (Motulsky and Ransnas, 1987) or Akaike information criteria (Akaike, 1974).

RESULTS

External Protons Reduce Single Channel Current Amplitude and Channel Mean Open Time

The effects of external proton concentration on single cardiac sodium channel currents are illustrated in Fig. 1. Representative single channel current records are shown from separate cell-attached patches at different values of external pH in response to depolarizing voltage steps to a test potential of −40 mV. Each panel shows six consecutive single channel records followed by the corresponding ensemble-averaged current.

At a normal external pH (7.4) the channel opens rapidly in response to depolarization, and openings are clustered at the beginning of the depolarization due to rapid activation and inactivation. Upon increasing the external proton concentration

(clockwise), there is a pronounced reduction in single channel current amplitude. In addition, Na channels tend to open later in the pulse and the time course of inactivation of the ensemble-averaged currents (τ_h) is prolonged, suggesting that channel gating is altered. Upon decreasing the proton concentration ($pH_o = 8.5$) there is an increase in single channel current amplitude. The effect of protons on channel gating will be discussed in more detail later.

A dose–response curve for the effect of protons on single channel current amplitude at a test potential of −40 mV is shown in Fig. 2. Single channel current

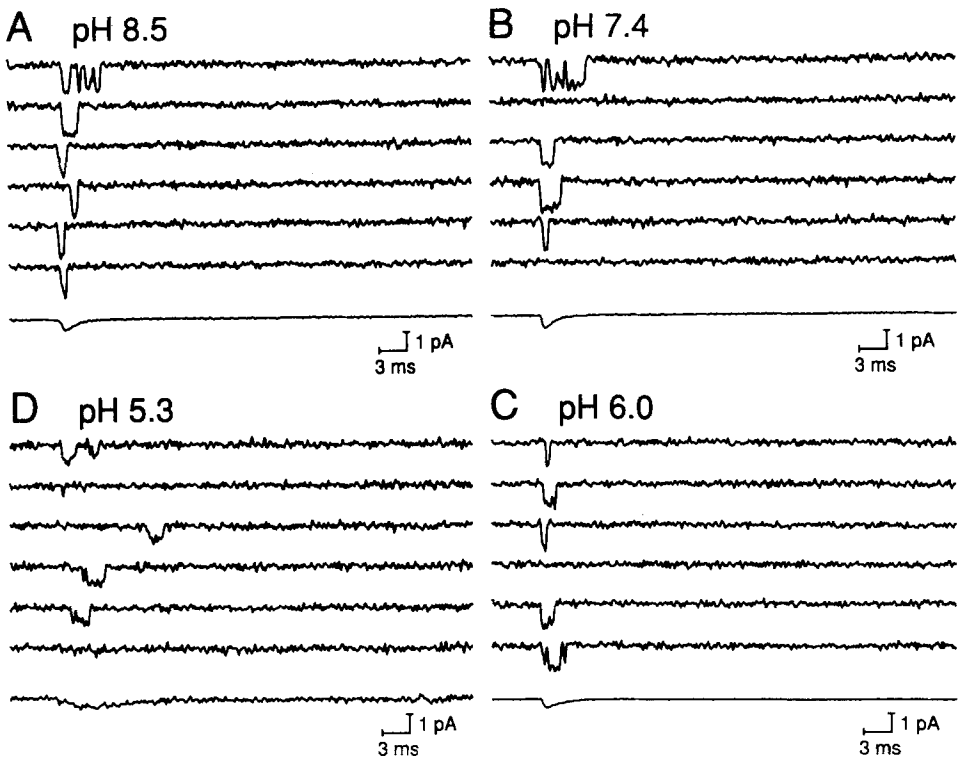

FIGURE 1. Effect of external H^+ on single sodium channels. Single sodium channel records were obtained at four different values of pH_o. Each panel has six consecutive sweeps followed by the corresponding ensemble-averaged current. The calibration for the ensemble-averaged current obtained at pH_o 5.3 is 0.25 pA. The test potential is −40 mV. (*A*) $V_h = -110$ mV. (*B* and *D*) $V_h = -120$ mV. (*C*) $V_h = -98$ mV.

amplitude shows a sigmoidal dependence on proton concentration that approximately follows the simple channel block scheme (model 1, solid curve), although the model predicts a somewhat steeper relation between pH_o and single channel current than is observed. As will be discussed later, better fits to the data can be obtained after taking into account surface potential effects (see Fig. 2). The best fit of model 1 yields a maximal single channel current amplitude of 1.50 pA and an apparent pK_H^* of 5.04, similar to previously reported pK values for inhibition by protons of maximal

macroscopic sodium conductance (Hille, 1968; Mozhayeva and Naumov, 1983; Yatani et al., 1984).

How do protons reduce the single channel current amplitude? One possible mechanism is that protons act as fast channel blockers, which will lead to an apparent decrease in single channel amplitude if blocking and unblocking events are much faster than the 2-kHz bandwidth of our recordings. According to Woodhull's simple model, protons bind to a site within the membrane electric field and so the fast blocking events are expected to be voltage dependent, with less block observed at more positive potentials. To evaluate this possibility, we measured the effects of external protons on single channel current at different test potentials.

Fig. 3 *A* shows single channel *i-V* curves at different values of external pH obtained from separate patches. Increasing the external proton concentration reduces single channel current amplitude over the entire voltage range tested, between −70 and −20 mV (the range of membrane potentials where it is possible to measure i with a

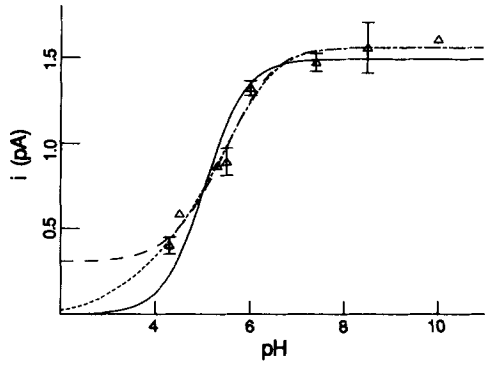

FIGURE 2. Dose–response curve for block of Na^+ current by external H^+. Mean single channel current (mean ± SD) is plotted as a function of pH_o and fitted by the simple one-to-one binding scheme of model 1 (solid curve, Eq. 5) with a pK_H^* of 5.04 and an i_{max} of 1.50 pA. Data points are averages from 2–13 separate experiments. The narrow dashed curve is the best fit by model 2, which includes the effect of surface charge on the local proton concentration. The fit yields the following values: pK_H 3.76, pK_H^* 3.87, σ_t −1e/52 Å^2, and i_{max} 1.57 pA. The broad dashed curve is the best fit of model 3A, yielding a σ_t of −1e/360 Å^2, a pK_H of 4.72, and a minimum channel current amplitude of 0.31 pA. See the text for details about models.

reasonable signal/noise ratio). To evaluate possible voltage-dependent block, we normalized the single channel current amplitude at pH_o 5.5 by its value at pH_o 7.4 and plotted the ratio as a function of test potential. As shown in Fig. 3 *B*, the curve is quite flat over this 50-mV range. A straight line fit by linear regression suggests a possible slight increase in block upon depolarization, opposite to the prediction of Woodhull's simple model (although consistent with more complicated channel block models such as Begenisich and Danko, 1983).

Protons could cause a voltage-dependent reduction in macroscopic sodium current if they bound to a second site within the channel, where they might act as slow channel blockers. In this case, protons should cause a concentration-dependent reduction in channel open time. Fig. 4 shows that raising the external proton concentration reduces τ_o from 0.77 ms at pH_o 7.4 to 0.3 ms at pH_o 4.5. However, neither the proton concentration dependence nor the voltage dependence of this effect is consistent with simple channel block. Thus, if protons act as slow channel

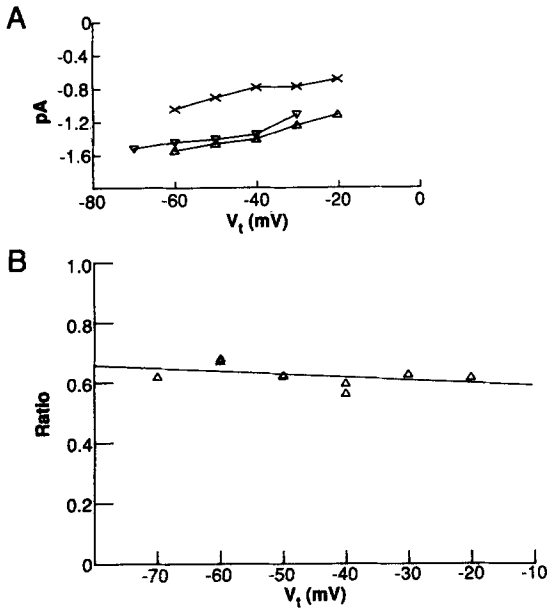

FIGURE 3. Effect of external H^+ on single channel *i-V* curves. (*A*) *i-V* curves at different values of pH_o. *Triangles*, pH_o 7.4; *inverted triangles*, pH_o 6.0; *crosses*, pH_o 5.5. (*B*) The ratio of the current amplitude (*i*) at pH_o 5.5 to that at pH_o 7.4 is plotted as a function of V_t and fitted by a linear function. Data points are from individual experiments.

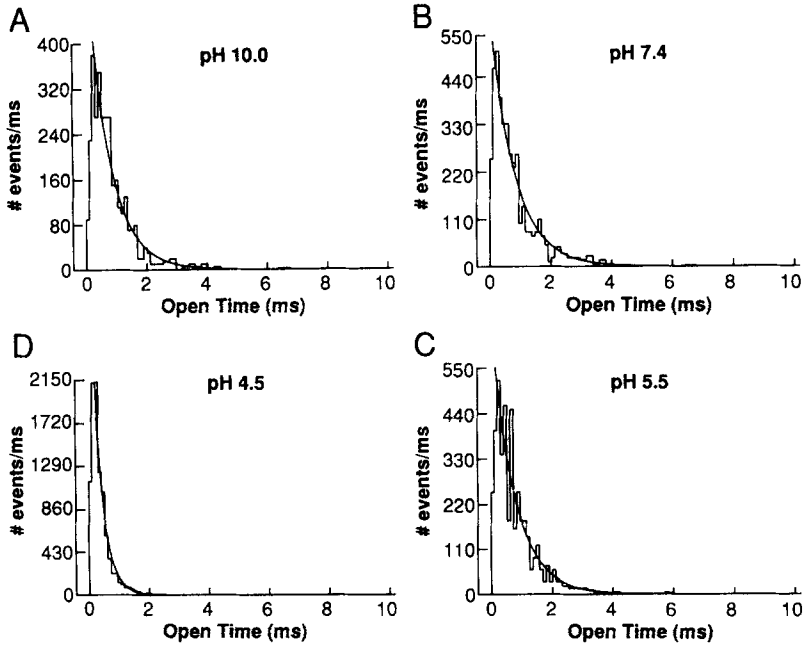

FIGURE 4. Channel open time histograms at four different pH_o values. The test potential is −40 mV. The histograms are fitted by a single exponential function to estimate the channel mean open time τ_o. (*A*) V_h = −100 mV, τ_o = 0.69 ms. (*B*) V_h = −103 mV, τ_o = 0.76 ms. (*C*) V_h = −98 mV, τ_o = 0.71 ms. (*D*) V_h = −110, τ_o = 0.30 ms.

blockers, channel open time should obey the relation $1/\tau_o' = 1/\tau_o + [H^+] \cdot k_f$, where τ_o' is the open time at a given proton concentration $[H^+]$, τ_o is the open time with no channel block, and k_f is the forward rate constant for channel block. This predicts a sigmoidal relationship when τ_o is plotted as a function of pH_o, which contrasts with the data of Fig. 5 *A*, where τ_o reaches a peak value at pH_o 7.4 and then declines from this peak at higher pH_o.

A possible explanation for this complicated dose–response relation is suggested by the data of Fig. 5 *B*, which plots τ_o as a function of membrane voltage at different values of pH_o. As previously reported (Grant and Starmer, 1987; Yue, Lawrence, and Marban, 1989; Berman et al., 1989), at pH_o 7.4 there is a nonmonotonic relation between τ_o and membrane potential, due to the opposite voltage dependencies of the

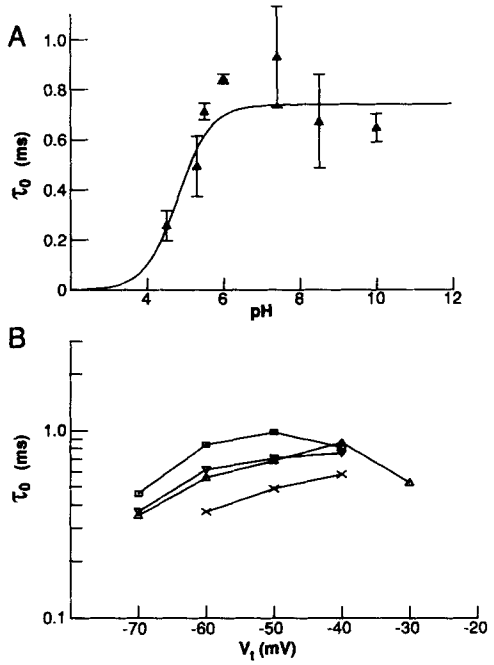

FIGURE 5. Effect of external H^+ on channel mean open time. (*A*) τ_o is plotted as a function of pH_o (mean ± SD). Data points are averages of 2–13 separate experiments. Test potential is −40 mV. The smooth curve is the best fit to the function: $1/\tau_o' = 1/\tau_o + [H] \cdot k_f$ (see text for details). (*B*) τ_o is plotted as a function of V_t at different pH_o. Data are from individual experiments. *Squares*, pH_o 7.4; *triangles*, pH_o 6.0; *inverted triangles*, pH_o 5.5; *crosses*, pH_o 5.3.

rate of open channel deactivation (the rate for return to a resting closed state; *a* in the terminology of Aldrich, Corey, and Stevens, 1983) and the rate of open channel inactivation (*b* in the terminology of Aldrich et al., 1983). Qualitatively, increasing the proton concentration appears to shift the relation between τ_o and voltage to more positive potentials. Such effects of pH_o are suggestive of changes in surface potential, as previously reported in many studies (see Hille, 1984).

External Protons Shift Cardiac Sodium Channel Gating

To assess further the possible surface potential effects of pH_o changes, we measured the effects of protons on ensemble-averaged sodium current inactivation and single channel activation kinetics.

Fig. 6 shows examples of steady-state inactivation (h_∞) curves obtained at different values of pH_o. The data have been fitted by standard Hodgkin-Huxley inactivation curves to obtain the midpoint of inactivation ($V_{1/2}$) and slope (k). As previously reported, protons cause a concentration-dependent shift of the h_∞ curves in the depolarizing direction. As pH_o decreases from 7.4 to 5.5, $V_{1/2}$ shifts by 13.3 mV, from -107.6 ± 2.6 (mean ± SD, $n = 16$) to -94.3 ± 1.85 mV ($n = 3$, $P < 0.001$). There is no significant change in the steepness of the curves.

Protons induce similar shifts in the voltage dependence of the apparent time constant of inactivation (τ_h) of ensemble-averaged sodium currents (Fig. 7). At pH_o 7.4 there is a voltage-dependent reduction in τ_h as the test potential is made more positive, in agreement with previous studies. As proton concentration increases, there is an increase in τ_h at all test potentials, with little change in the slope of the curve relating τ_h to test potential. Thus, protons appear to shift the relations between τ_h and V_m to more positive potentials. Relative to pH_o 7.4, the τ_h curve is shifted by ~9.8 mV at pH_o 6 and by 17.3 mV at pH_o 5.5.

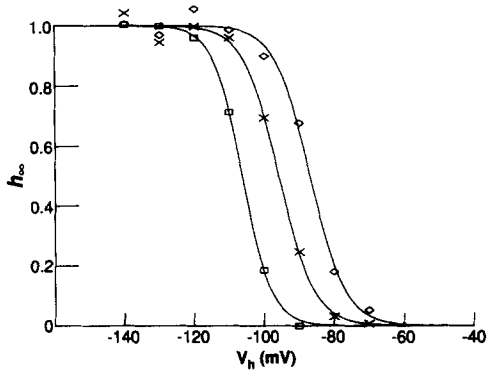

FIGURE 6. External H^+ shifts the steady-state inactivation curves of ensemble-averaged currents. Data are from individual experiments and are fitted by the standard Hodgkin-Huxley inactivation curve to estimate $V_{1/2}$ and slope (k). *Squares*, pH_o 7.4, $V_{1/2} = -106.25$ mV, $k = -4.14$; *crosses*, pH_o 5.5, $V_{1/2} = -95.78$ mV, $k = -5.00$; *diamonds*, pH_o 4.8, $V_{1/2} = -86.87$ mV, $k = -4.98$.

As the macroscopic rate constant τ_h depends on both activation kinetics and the rate of open channel inactivation (Aldrich et al., 1983), several different kinetic mechanisms could account for the increase in τ_h at low pH_o, including: (*a*) an increase in channel open time, (*b*) an increase in the number of channel openings and closings before inactivating, or (*c*) a slowing of the rate of channel activation. As protons actually decrease open time (Fig. 4), the increase in τ_h must reflect repeated openings and/or slowed activation. These two possibilities are addressed next.

The rate of channel activation was determined using cumulative first latency to opening histograms. Fig. 8 shows examples of such histograms, which plot the probability, $P_1(t)$, that a channel opens for the first time during a sweep after a given time, t, for four different values of pH_o at a constant test potential of −40 mV. The first latency distribution is fitted by the sum of two exponential components, with the slow component being dominant. The time constant of the slow exponential component (τ_s) shows a clear increase with proton concentration. For the patches in Fig. 8, there is a seven-fold increase in τ_s as pH_o decreases from 7.4 to 5.3. Fig. 8 *C* summarizes the effect of protons on τ_s at different membrane potentials. The data are from individual experiments. Protons prolong τ_s at a given membrane potential,

and the overall effect is to shift the τ_s vs. voltage relation to more positive potentials, as observed above.

The effect of protons on the probability that a channel reopens is addressed by examining the conditional probability $m(t)$ that a channel is open at any time t, given that it first opens at time $t = 0$. Fig. 9 shows such plots obtained from three separate patches at pH_o 8.5, 7.4, and 5.3. Each of the patches has only one functional channel. Panels *A–C* show the channel open time distribution superimposed on the corresponding $m(t)$ distribution. If a channel opens only once during a pulse, $m(t)$ will be identical to the open time distribution, $o(t)$. If a channel opens more than once, $m(t)$ will decay more slowly than $o(t)$. When the open time distributions are compared with $m(t)$, it is clear that either increasing or decreasing external proton concentration from the normal value (pH 7.4) significantly increases the probability of repeated openings. While at pH_o 7.4 $m(t)$ nearly superimposes on $o(t)$, indicating that the sodium channels tend to open only once during a depolarization, at either pH_o 5.3 or 8 $m(t)$ decays much more slowly than the open time distribution. Direct measurements show that the mean number of openings per sweep increases from 1.1 at pH_o

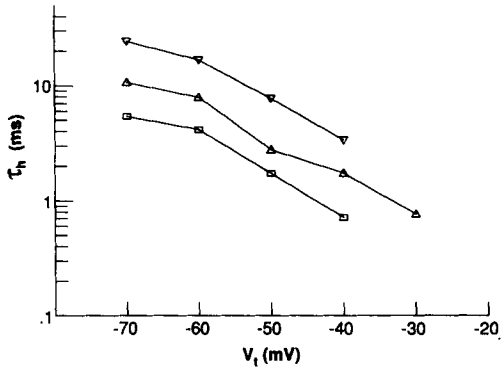

FIGURE 7. External H^+ prolongs the time constant of inactivation (τ_h) of ensemble-averaged current. τ_h is plotted as a function of V_t at different pH_o. *Squares*, pH_o 7.4; *triangles*, pH_o 6.0; *inverted triangles*, pH_o 5.5. Data are from individual experiments.

7.4 to 2.5 at pH_o 5.3. Thus, the increase in τ_h at low pH is due to both a decrease in the rate of activation and an increase in the probability that a channel reopens. Both of these effects of low pH_o (i.e., increased τ_h and repeated openings) are what is observed at normal pH_o (7.4) at test potentials negative to −40 mV, supporting the idea that protons cause a depolarizing voltage shift in channel gating (Berman et al., 1989; Yue et al., 1989). However, the increased reopenings at high pH are less readily explained by a simple surface potential effect.

From the dose–response relation between voltage shifts in channel gating and proton concentration, quantitative information about the proton binding site can be obtained. We have focused on the effects of protons on the midpoint of the steady-state inactivation–voltage relation as this parameter is the most reliably measured. Fig. 10 shows that the dose–response curve for the shift by protons in the $V_{1/2}$ of steady-state inactivation (squares) is well fit by a Gouy-Chapman-Stern model (solid curve) (Eqs. 2–4). The fitted curve yields estimates for the pK_H of the binding site for protons of 5.16 and a value for the total surface charge density of $-1e/490$ Å^2, which predict a surface potential of around −30 mV at the normal external pH of 7.4.

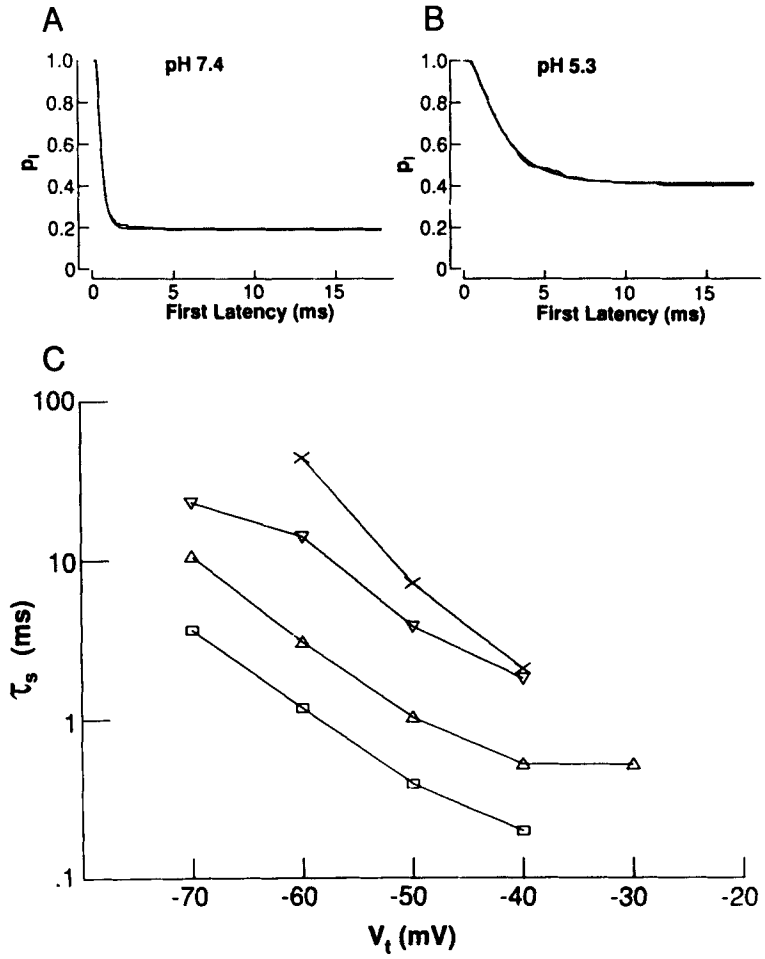

FIGURE 8. First latency distributions at different pH_o. Test potential is −40 mV. Cumulative histograms (*A* and *B*) show probability P_1 that a channel opening first occurs later than time *t*. The smooth curve is the best fit of a two-exponential function, yielding the fast (τ_f) and slow (τ_s) components, as well as probability that a resting channel does not open during pulse, P(ss). At pH_o 7.4 (*A*), τ_f is 0.12 ms, τ_s is 0.31 ms, and P(ss) is 0.178. As pH_o decreases, τ_s becomes longer. At pH_o 5.3 (*B*), τ_f is 0.54 ms, τ_s is 2.10 ms, and P(ss) is 0.407. *C* plots τ_s as a function of V_t at different pH_o. Data are from individual experiments. *Squares*, pH_o 7.4; *triangles*, pH_o 6.0; *inverted triangles*, pH_o 5.5; *crosses*, pH_o 5.3.

Surface Potential Theory vs. Block Theory: Model Fitting

Surface charge effects offer a possible explanation for why the dose–response curve for the reduction of single channel current amplitude by protons (Fig. 2) deviates from the simple channel block model (model 1). At high pH_o the negative surface potential will lead to a higher local cation concentration near the membrane due to electrostatic attraction. As the bulk proton concentration increases, the local proton concentration increases more slowly due to the titration of the surface charge, which reduces the negative surface potential. Alternatively, the reduction in single channel

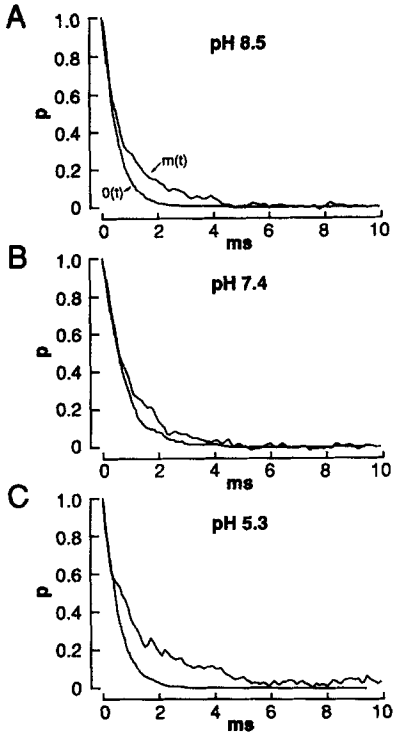

FIGURE 9. Effect of external H^+ on the probability of reopenings. Each panel plots the cumulative open time distribution $o(t)$ superimposed by the conditional probability distribution $m(t)$, the probability that the channel is open at time t given that it opens at $t = 0$ (see Methods). Each of the three patches shown here contained only one active channel. Test potential is −40 mV.

current with protons may not be due to channel block but may simply result from a decrease in the local external sodium concentration at the surface of the membrane due to the reduction in surface potential.

Fig. 2 compares fits to the single channel current dose–response data for the simple channel block (model 1, solid curve), channel block taking into account surface potential effects on local proton concentration (model 2, dotted curve), and

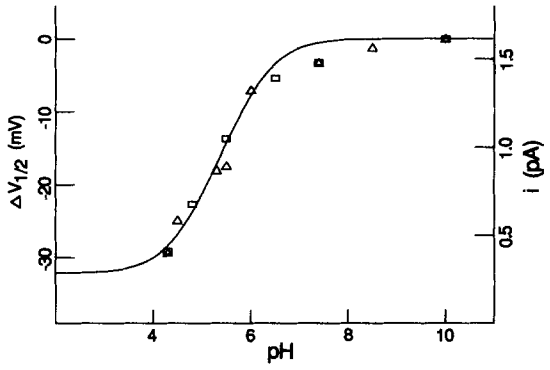

FIGURE 10. Shift of the midpoint of the steady-state inactivation curve ($V_{1/2}$) by external H^+. Data points (*squares*) represent the differences in $V_{1/2}$ between those obtained at lower pH_o and that at pH_o 10.0, fitted by Eqs. 2–4. The smooth curve represents the best fit, which yields a pK_H of 5.16 and a σ_t of −1e/490 Å^2. Superimposed on this fit are the mean values of single channel current amplitude at different pH_o (*triangles, right-hand axis,* scaled so that maximal current at high pH superimposes on $V_{1/2}$).

surface potential effects on local Na concentration with no direct proton block (model 3A, dashed curve). Models 2 and 3 provide a visually and statistically significant better fit to the data than does the simple channel block model 1 ($P < 0.05$ for model 2, $P < 0.005$ for model 3A). A least-squares best fit of model 2 yields a total surface charge density of $-1e/52$ Å^2, a pK_H of 3.76, a pK_H^* of 3.87, and a maximal single channel amplitude of 1.57 pA (at -40 mV). The best fit of model 3A yields a lower estimate for total surface charge density of $-1e/360$ Å^2, a higher pK_H of 4.72, and a minimum single channel amplitude of 0.31 pA (at $V_t = -40$ mV). The total charge density (yielding a membrane surface potential of -40.7 mV at pH_o 7.4) and pK_H derived from model 3A are close to those obtained by the independent fit to the shift of $V_{1/2}$ of steady-state inactivation in Fig. 10. The surface Na concentration model 3B (Eqs. 2–4 and 7, which uses the Goldman-Hodgkin-Katz equation to estimate i) yields a pK_H of 4.67 and a σ_t of $-1e/85$ Å^2, but the fit is not statistically better than that of model 1 ($P > 0.05$). Also, a combined channel block–surface Na concentration model (models 2 and 3A) does not yield a statistically better fit compared with models 2 or 3A alone.

The major difference between the predictions of models 2 and 3A is that at very low external pH, the local Na concentration model predicts a residual single channel current that will be independent of further increases in proton concentration (since all the surface charges eventually become titrated). In contrast, the modified block model predicts that the single channel amplitude will eventually be reduced to zero. Unfortunately, we cannot reliably measure single channel events at pH_o 4.0, where the two models begin to deviate, because the large positive voltage shift in gating at this pH_o prevents channels from activating using steps to -40 mV. Although the sum-squared deviation of model 3A is somewhat less than that of model 2, this difference is not statistically significant.

DISCUSSION

In this study, we have characterized the effects of external protons on single cardiac sodium channels. Our results confirm previous studies on macroscopic sodium current by showing that protons have two main effects on single sodium channel currents: they reduce single channel current amplitude and cause a positive shift in voltage-dependent gating.

Effects on Gating

External protons cause similar shifts in the voltage dependence of the time constant of macroscopic current inactivation, steady-state inactivation, microscopic rate of channel activation, and channel open time. These effects are consistent with the titration of external surface charges which leads to changes in surface potential and can be quantitatively described by a Gouy-Chapman-Stern surface charge model incorporating specific proton binding and charge screening. Fits of this model to titration curves for shifts in steady-state inactivation yield estimates for the K_H for the proton binding site and for σ_t, the total surface charge density, of 1.89×10^{-5} M and $-1e/360$ Å^2, respectively.

One major limitation of the Gouy-Chapman-Stern approach is that it assumes a uniform charge distribution on the membrane which affects the membrane electric

field, as expected if negatively charged phospholipid head groups were involved. However, studies in planar lipid bilayers suggest that the relevant surface charge may be on the channel itself, since membrane phospholipid charge does not appear to alter gating (Green, Weiss, and Andersen, 1987; Cuckierman, Zinkand, French, and Krueger, 1988). The similarity in surface charge density obtained by Ravindran and Moczydlowski (1989) for reconstituted sodium channels in artificial bilayers with our measurements in native membranes supports this idea.

We attempted to measure the effects of protons on the microscopic rates of open channel inactivation (*b*) and open channel closing (*a;* or rate of return to rest) using an Aldrich, Corey, and Stevens model (1983). Previous studies in cardiac muscle indicate that *a* and *b* show opposite voltage dependencies, with *a* decreasing and *b* increasing at more positive potentials (Grant and Starmer, 1987; Berman et al., 1989; Yue et al., 1989). Consistent with this voltage dependence, we find that lowering external pH below 7.4 leads to an increase in *a* and a decrease in *b*, as expected for a positive voltage shift. Raising the pH_o above 7.4, however, has the opposite effect from the expected negative voltage shift in that there is an increase in *a* and a decrease in *b*, leading to an increase in channel reopening during a depolarization (Fig. 9). This may indicate a separate specific role for an acidic amino acid residue in controlling channel gating that is not related to potential charge effects per se.

Effects on Single Channel Current Amplitude

Our results showing a reduction by protons of the single sodium channel current amplitude confirm the previous findings of Sigworth (1980) based on noise analysis, and probably underlie the well-characterized action of protons to reduce the maximal sodium conductance in macroscopic experiments. However, the mechanism responsible for the reduction in single channel current amplitude remains uncertain. Woodhull (1973) showed that the effect of protons on maximal sodium conductance could be relieved by depolarization and proposed that protons bind to a site within the channel, thereby blocking current flow. From the magnitude of the voltage dependence of blockade, Woodhull calculated that the binding site was located within the channel at a fractional electrical distance of 0.26 across the membrane electric field. Subsequently, similar results were obtained from different preparations, including nerve (Hille, Woodhull, and Shapiro, 1975; Begenisich and Danko, 1983; Mozhayeva et al., 1984) and cardiac muscle cells (Yatani et al., 1984).

A potential problem with such studies of macroscopic currents arises from possible effects of protons on sodium channel gating since the macroscopic peak current amplitude depends on channel open probability as well as on channel open conductance. Thus, Campbell (1982) concluded that block by protons was voltage independent and that the apparent voltage dependence of block from peak sodium current measurements was due to a second action of protons to alter channel kinetics (although cf. Begenisich and Danko, 1983).

By using single channel recording, we have directly determined the effects of protons on channel gating and channel conductance independently. Our results clearly show a dose-dependent decrease of single channel current amplitude by protons, consistent with a reduction in channel conductance. Similar effects of external protons to reduce single channel current amplitude have recently been

reported for brain (Daumas and Anderson, 1991) and cardiac (Backx, Marban, and Yue, 1990; Backx and Yue, 1991) sodium channels. We find that the effects of protons on single channel current amplitude do not show any significant dependence on membrane potential over a 50-mV range between −70 and −20 mV (see Figs. 2 and 3). This argues against the simplest model of Woodhull, where external protons bind to a blocking site within the channel and do not permeate. We cannot rule out a more complicated scheme proposed by Woodhull where protons can permeate the channel at negative voltages. Begenisich and Danko (1983) have shown that in squid giant axon proton block is well described by such a model incorporating proton permeation. Moreover, their Fig. 8 shows that over the voltage range of our measurements, there is a relatively flat relationship between membrane potential and block, with block actually increasing slightly upon depolarization from −70 to −20 mV. Relief of block only occurs at positive potentials, where we cannot readily resolve single sodium channels. Similar results for cardiac sodium channels have recently been presented (Backx and Yue, 1991).

Studies on the effects of external protons on calcium channels have also reported a voltage-independent reduction in single channel current, although the mechanism by which protons reduce single calcium channel current, involving induction of a subconductance state, is different from the effects reported here (Prod'hom, Pietrobon, and Hess, 1987, 1989; Pietrobon, Prod'hom, and Hess, 1989). As protonation of the calcium channel does not appreciably change the surface potential near the entry of the permeation pathway, the authors conclude that protonation changes the channel conformation such that the channel is less permeable to calcium.

A second model for the reduction in maximal sodium conductance was proposed by Drouin and Neumcke (1974), who suggested that protons inhibited sodium current by two independent mechanisms: (*a*) protons blocked the channel in a voltage independent manner at an external site on the channel; and (*b*) protons titrated negative surface charges at a second membrane site, leading to a reduction in local sodium concentration and reduction in sodium conductance. We have found that our data can be well fitted by a simpler model in which the reduction in single channel current is due solely to changes in local Na concentration due to changes in surface potential (model 3A).

Can we distinguish between channel block and surface charge effects? Simply fitting the dose–response curve for the reduction in current amplitude with protons does not adequately distinguish between channel block (model 2) and local sodium concentration effects (model 3A), since both models provide similarly good fits. However, the total charge density ($-1e/52$ Å^2) derived from the modified block model (model 2) is much higher than previously reported surface charge densities for a variety of channels in different membranes (McLaughlin, 1977; Hille, 1984), where estimates of surface charge density range from $-1e/100$ Å^2 to $-1e/500$ Å^2. For example, in rat cardiac ventricular cells, Krafte and Kass (1988) estimated, from shifts in $V_{1/2}$ of L-type calcium current inactivation, a surface charge density of $-1e/250$ Å^2 and a pK of 5.8. Cardiac sodium channels reconstituted in planar lipid bilayers also show a low charge density of $-1e/450$ Å^2 (Ravindran and Moczydlowski, 1989). The surface charge density of $-1e/360$ Å^2 obtained from fits of the local Na concentration model (3), in contrast, is in much better agreement with previous studies and with our

surface charge estimates obtained from effects of pH_o on channel inactivation gating, which yield a surface charge density of $-1e/490$ Å^2 and a pK of 5.16.

The similarity we find between surface charge density and pK values obtained from inactivation gating and single channel current amplitude measurements suggests that the effects of protons on both processes may reflect the titration of a single class of negatively charged sites. This similarity is clearly shown in Fig. 10, which superimposes the dose–response curves for reduction in single channel current amplitude (triangles) and the shift in the $V_{1/2}$ of inactivation (squares) by protons. While this similarity could be coincidental, combined with the lack of voltage-dependent block by protons (Fig. 3), it suggests that the reduction in single channel current may be due to reduction in local $[Na^+]_o$ rather than to channel block.

Recent evidence in favor of channel block by protons comes from Backx et al. (1990), who report that protons reduce single channel current amplitude and increase open channel noise in cardiac sodium channels modified by DPI 201-106 (which induces long open states; Nilius, Vereecke, and Carmeliet, 1989). These authors suggest that the increased noise represents rapid channel block, although rapid changes in local surface potential would also cause rapid changes in local Na^+ concentration and produce a similar increase in noise. Backx and Yue (1991) showed that in cardiac Na^+ channels modified by fenvalerate (which slows deactivation), the decrease in single channel current by protons is enhanced at very positive voltages and relieved at negative voltages. While this finding indicates that the proton binding site lies within the channel, it does not distinguish whether protons act by physically blocking the channel or by reducing local $[Na^+]_o$ in the channel through a surface charge effect. The brief openings of unmodified cardiac sodium channels prevented us from making similar measurements. Site-directed mutagenesis of negative charges around the mouth of the sodium channel (e.g., Noda, Suzuki, Numa, and Stuhmer, 1989) will be useful in determining the exact site or sites of proton action.

We thank Dr. Olaf Andersen for helpful suggestions on surface charge effects and Dr. Ofer Binah for the preparation of guinea pig ventricular myocytes.

This work was supported by NIH grant HL-30557.

Original version received 7 February 1991 and accepted version received 12 June 1991.

REFERENCES

Akaike, H. 1974. A new look at the statistical model identification. *IEEE Transactions on Automatic Control.* 19:716–723.

Aldrich, R. W., D. P. Corey, and C. F. Stevens. 1983. A reinterpretation of mammalian sodium channel gating based on single channel recording. *Nature.* 306:436–441.

Backx, P. H., E. Marban, and D. T. Yue. 1990. Flicker block of cardiac Na channels by Cd^{2+} and protons. *Biophysical Journal.* 57:298*a*. (Abstr.)

Backx, P. H., and D. T. Yue. 1991. Proton permeation through cardiac sodium channels. *Biophysical Journal.* 59:26*a*. (Abstr.)

Begenisich, T., and M. Danko. 1983. Hydrogen ion block of the sodium pore in squid giant axons. *Journal of General Physiology.* 82:599–618.

Berman, M. F., J. S. Camardo, R. B. Robinson, and S. A. Siegelbaum. 1989. Single sodium channels

from canine ventricular myocytes: voltage dependence and relative rates of activation and inactivation. *Journal of Physiology.* 415:503–531.

Binah, O., I. Rubinstein, and E. Gilat. 1987. Effects of thyroid hormone on the action potential and membrane currents of guinea pig ventricular myocytes. *Pflügers Archiv.* 409:214–216.

Campbell, D. T. 1982. Do protons block Na^+ channels by binding to a site outside the pore? *Nature.* 298:165–167.

Colquhoun, D., and F. J. Sigworth. 1983. Fitting and statistical analysis of single-channel records. *In* Single Channel Recording. B. Sakmann and E. Neher, editors. Plenum Publishing Corp., New York and London. 191–263.

Cukierman, S., W. C. Zinkand, R. J. French, and B. K. Krueger. 1988. Effects of membrane surface charge and calcium on the gating of rat brain sodium channels in planar bilayers. *Journal of General Physiology.* 92:431–447.

Daumas, P., and O. S. Anderson. 1991. Titrating the conductance of BTX-modified brain sodium channel. *Biophysical Journal.* 59:259*a*. (Abstr.)

Dorn, W. S., and D. D. McCracken. 1972. Numerical Methods with Fortran IV Case Studies. John Wiley & Sons, Inc., New York. 25–29.

Drouin, H., and B. Neumcke. 1974. Specific and unspecific charges at the sodium channels of the nerve membrane. *Pflügers Archiv.* 351:207–229.

Drouin, H., and R. The. 1969. The effect of reducing extracellular pH on the membrane currents of the Ranvier node. *Pflügers Archiv.* 313:80–88.

Grahame, D. C. 1947. The electrical double layer and the theory of electrocapillarity. *Chemical Reviews.* 41:441–501.

Grant, A. O., and C. F. Starmer. 1987. Mechanisms of closure of cardiac sodium channels in rabbit ventricular myocytes: single-channel analysis. *Circulation Research.* 60:897–913.

Green, W. N., and O. S. Andersen. 1991. Surface charges and ion channel function. *Annual Review of Physiology.* 53:341–359.

Green, W. N., L. B. Weiss, and O. S. Andersen. 1987. Batrachotoxin-modified sodium channels in planar lipid bilayers. Ion permeation and block. *Journal of General Physiology.* 89:841–872.

Hamill, O. P., E. Marty, E. Neher, B. Sakmann, and F. J. Sigworth. 1981. Improved patch-clamp techniques for high-resolution current recording from cells and cell-free membrane patches. *Pflügers Archiv.* 391:85–100.

Hille, B. 1968. Charges and potentials at the nerve surface. Divalent ions and pH. *Journal of General Physiology.* 51:221–236.

Hille, B. 1984. Ionic Channels of Excitable Membranes. Sinauer Associates, Inc., Sunderland, MA. 426 pp.

Hille, B., A. M. Woodhull, and B. I. Shapiro. 1975. Negative surface charge near sodium channels of nerve: divalent ions, monovalent ions, and pH. *Philosophical Transactions of the Royal Society of London, Series B.* 270:301–318.

Isenberg, G., and U. Klockner. 1982. Calcium-tolerant ventricular myocytes prepared by preincubation in a "KB medium." *Pflügers Archiv.* 395:6–18.

Krafte, D. S., and R. S. Kass. 1988. Hydrogen ion modulation of Ca channel current in cardiac ventricular cells. Evidence for multiple mechanisms. *Journal of General Physiology.* 91:641–657.

McLaughlin, S. 1977. Electrostatic potentials at membrane-solution interfaces. *Current Topics in Membranes and Transport.* 9:71–144.

Motulsky, H. J., and L. A. Ransnas. 1987. Fitting curves to data using nonlinear regression: a practical and nonmathematical review. *FASEB Journal.* 1:365–374.

Mozhayeva, G. N., and A. P. Naumov. 1983. The permeability of sodium channels to hydrogen ions in nerve fibers. *Pflügers Archiv.* 396:163–173.

Mozhayeva, G. N., A. P. Naumov, and E. D. Nosyreva. 1984. A study on the potential-dependence of proton block of sodium channels. *Biochimica et Biophysica Acta.* 775:435–440.

Nilius, B., J. Vereecke, and E. Carmeliet. 1989. Properties of bursting Na channel in the presence of DPI 201-106 in guinea-pig ventricular myocytes. *Pflügers Archiv.* 413:234–241.

Noda, M., H. Suzuki, S. Numa, and W. Stuhmer. 1989. A single point mutation confers tetrodotoxin and saxitoxin insensitivity on the sodium channel II. *FEBS Letters.* 259:213–216.

Pietrobon, D., B. Prod'hom, and P. Hess. 1989. Interactions of protons with single open L-type calcium channels. *Journal of General Physiology.* 94:1–21.

Prod'hom, B., D. Pietrobon, and P. Hess. 1987. Direct measurement of proton transfer rates to a group controlling the dihydropyridine-sensitive Ca^{2+} channel. *Nature.* 333:373–376.

Prod'hom, B., D. Pietrobon, and P. Hess. 1989. Interactions of protons with single open L-type calcium channels. *Journal of General Physiology.* 94:23–42.

Ravindran, A., and E. Moczydlowski. 1989. Influence of negative surface charge on toxin binding to canine heart Na channels in planar bilayers. *Biophysical Journal.* 55:359–365.

Sigworth, F. J. 1980. The conductance of sodium channels under conditions of reduced current at the node of Ranvier. *Journal of Physiology.* 307:131–142.

Woodhull, A. M. 1973. Ionic blockage of sodium channels in nerve. *Journal of General Physiology.* 61:687–708.

Yatani, A., A. M. Brown, and N. Akaike. 1984. Effect of extracellular pH on sodium current in isolated, single rat ventricular cells. *Journal of Membrane Biology.* 78:163–168.

Yue, D. T., J. H. Lawrence, and M. Marban. 1989. Two molecular transitions influence cardiac sodium channel gating. *Science.* 244:349–352.

Zhang, J. F., and S. A. Siegelbaum. 1990. Effects of external pH on cardiac sodium channels. *Biophysical Journal.* 57:104*a*. (Abstr.)